

The Skin's Barrier: A Cryo-EM Based Overview of its Architecture and Stepwise Formation



JID Open

Lars Norlén^{1,2,3}, Magnus Lundborg^{4,5}, Christian Wennberg^{4,5}, Ali Narangifard^{4,5} and Bertil Daneholt^{2,5}

A major role of the skin is to serve as a barrier toward the environment. The skin's permeability barrier consists of a lipid structure positioned in the stratum corneum. Recent progress in high-resolution cryo-electron microscopy (cryo-EM) has allowed for elucidation of the architecture of the skin's barrier and its stepwise formation process representing the final stage of epidermal differentiation. In this review, we present an overview of the skin's barrier structure and its formation process, as evidenced by cryo-EM.

Journal of Investigative Dermatology (2022) **142**, 285–292; doi:10.1016/j.jid.2021.06.037

Introduction (Figure 1)

Investigation of the skin's permeability barrier dates back to the mid 19th century. For an in-depth background to the field, the interested reader is referred to a number of seminal papers (Berenson and Burch, 1951; Blank, 1952; Bouwstra et al., 1998, 1991; Brody, 1966; Duriau, 1856; Elias, 1983; Elias and Friend, 1975; Forslind, 1994; Homolle, 1853; Onken and Moyer, 1963; Potts and Guy, 1992; Scheuplein and Blank, 1971; Wertz and Downing, 1983; Winsor and Burch, 1944) and reviews (Feingold and Elias, 2014; Rabionet et al., 2014; Schaefer and Redelmeier, 1996; Schmitt and Neubert, 2018; van Smeden et al., 2014; Wertz, 2018).

Human skin serves to uphold homeostasis by preventing water loss from the body as well as by preventing the permeation of exogenous substances into the body. The major physical barrier property is located in the skin's topmost epidermal layer—the stratum corneum. It consists of a lipid structure positioned intercellularly between cornified dead cells.

The formation of the skin's barrier represents the final stage of epidermal differentiation. The epidermal cells move from the basal layer, through several layers of cells evolving into secretory cells, to the stratum corneum with cornified cells. Barrier formation is initiated in the topmost secretory cell

layers—the stratum granulosum (SG) (Figure 1, right column). The barrier lipids are synthesized in the endoplasmic reticulum and Golgi apparatus. They subsequently appear as a partly granular (green pattern) and partly lamellar (blue pattern) material inside an extensive tubuloreticular (lamellar body) membrane system (green pattern) (den Hollander et al., 2016; Elias et al., 1998; Yamanishi et al., 2019). The lipids are finally discharged into the intercellular space at the interface between SG and stratum corneum. Once in the stratum corneum intercellular space, the secreted lipids transform into laterally extended, stacked sheets (brown, pink, and yellow patterns), a process completed at the third to fifth stratum corneum layer. The stacked sheets are then observed in the intercellular space throughout the stratum corneum.

Discharge of lamellar lipid precursors from the apical side of SG2 cells has so far not been observed in human skin with cryo-electron microscopy (cryo-EM).

Electron microscopy (EM) visualizations of the stacked sheets came with Breathnach et al. (1973) and Elias and Friend (1975). Madison et al. (1987) further pioneered EM visualization by the introduction of ruthenium tetroxide (RuO_4) staining. In this way, the stacked sheets' characteristic broad-narrow-broad electron-lucent band staining pattern was discovered (Hou et al., 1991; Madison et al., 1987).

EM investigation of the tubuloreticular (lamellar body) membrane system and the barrier formation process, using conventional EM techniques, goes back to the mid-1960s (Brody, 1989; Elias et al., 1998; Fartasch, 1997; Landmann, 1986; Lavker, 1976; Madison et al., 1998; Matoltsy, 1966; Odland and Holbrook, 1981; Yamanishi et al., 2019).

In our laboratory, we have applied cryo-EM of vitreous sections (CEMOVIS) to elucidate *in situ* the molecular organization and the formation process of the skin's barrier structure (den Hollander et al., 2016; Iwai et al., 2012; Lundborg et al., 2018a; Narangifard et al., 2021, 2018; Wennberg et al., 2018). In cryo-EM, the tissue is preserved down to the molecular level at near-native conditions (Al-Amoudi et al., 2004; Dubochet et al., 1988). In the analysis of the cryo-EM images, atomic-detail molecular models subject to molecular dynamics (MD) simulation followed by EM simulation is employed. The image analysis procedure comprises the following three steps: (i) construction of candidate molecular models, (ii) generation of simulated electron micrographs on the basis of these models, and (iii) finally a comparison of the observed cryo-electron micrographs with the simulated ones.

Barrier formation

Cryo-EM patterns of the barrier formation process (Figure 2). During epidermal differentiation, the skin's barrier structure undergoes five apparent maturation stages

¹Department of Medicine, Solna, Karolinska Institute, Stockholm, Sweden;

²Department of Cell and Molecular Biology, Karolinska Institute, Stockholm, Sweden; ³Dermatology Clinic, Karolinska University Hospital, Stockholm, Sweden; and ⁴Science for Life Laboratory, ERCO Pharma AB, Stockholm, Sweden

⁵These authors contributed equally

Correspondence: Lars Norlén, Department of Cell and Molecular Biology, Karolinska Institute, Biomedicum, 17177 Stockholm, Sweden. E-mail: lars.norlen@ki.se

Abbreviations: CEMOVIS, cryo-electron microscopy of vitreous sections; cryo-EM, cryo-electron microscopy; EM, electron microscopy; MD, molecular dynamics; RuO_4 , ruthenium tetroxide; SG, stratum granulosum

Received 27 April 2021; revised 28 June 2021; accepted 30 June 2021; corrected proof published online 31 August 2021

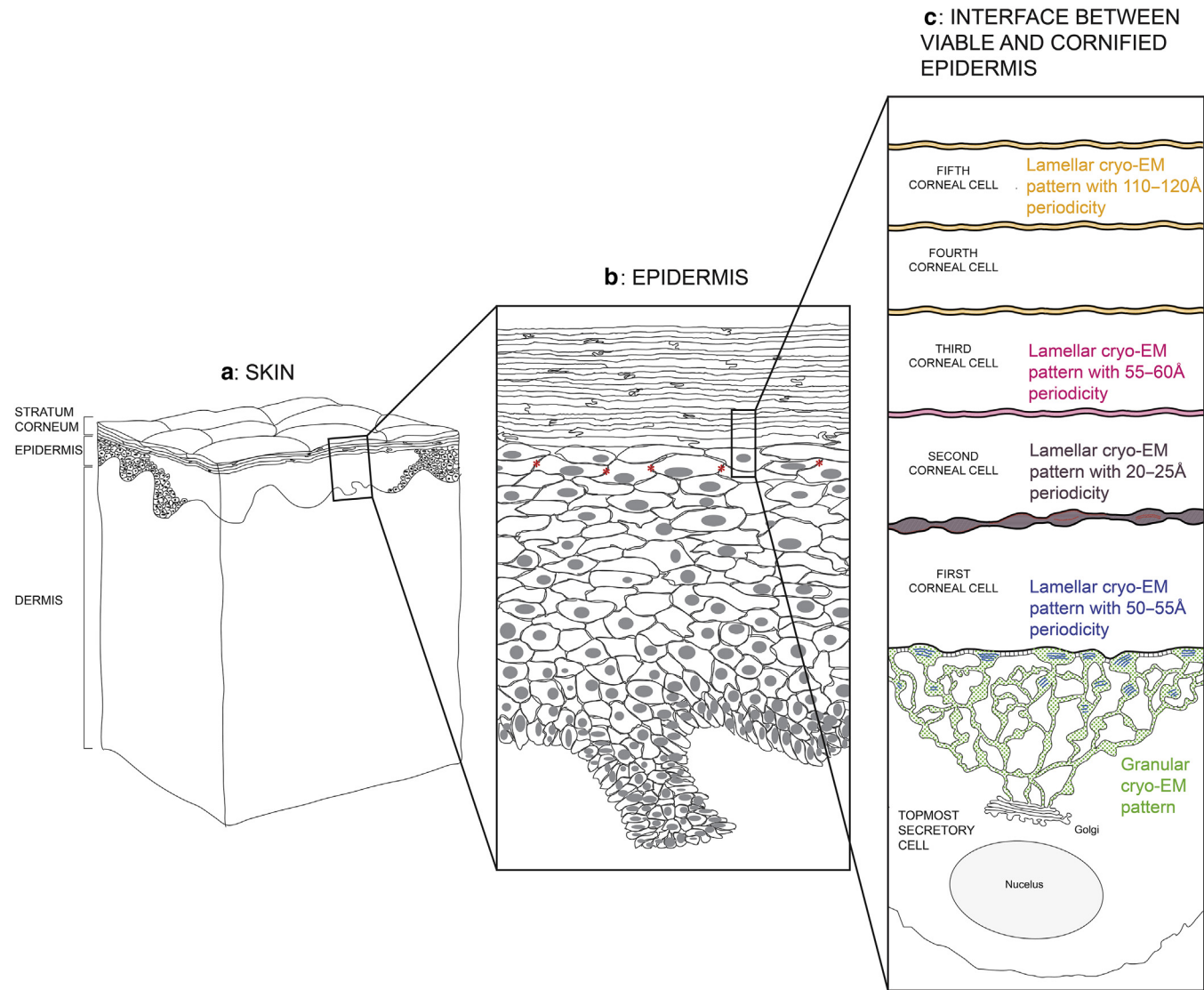


Figure 1. Schematic view of the skin. (a) Left column: full-thickness skin; (b) middle column: epidermis; (c) right column: interface between viable and cornified epidermis. The green and blue areas indicate the tuboluretticular (lamellar body) network of a secretory (SG) cell; the dark brown area indicates intercellular space between the first and second corneal (stratum corneum) cells; the pink area indicates the intercellular space between the second and third corneal cells; and the yellow area indicates the intercellular spaces above the third corneal cell. (c) Desmosomes connecting the secretory cell to the first corneal cell are indicated by transverse striations (black). (b) Tight junctions in the SG cell periphery (Yokouchi et al., 2016) are indicated by stars (red). cryo-EM, cryo-electron microscopy; SG, stratum granulosum.

represented by five different cryo-EM patterns: (i) a granular pattern (Figure 2a), (ii) a lamellar pattern with 50–55 Å periodicity (Figure 2b), (iii) a lamellar pattern with 20–25 Å periodicity (Figure 2c), (iv) a lamellar pattern with 55–60 Å periodicity (Figure 2d), and (v) a lamellar pattern with 110–120 Å periodicity (Figure 2e).

The five stages identified in the barrier formation process (Figure 3). Analysis of the five cryo-EM patterns using MD model building combined with EM simulation suggests that the granular pattern represents a highly folded and highly hydrated conventional skin lipid bilayer (Figure 3a) (Narangifard et al., 2018), that the lamellar pattern with 50–55 Å periodicity represents a stacked skin lipid monolayer with mixed hairpin and splayed ceramides (Figure 3b) (Narangifard et al., 2018), that the lamellar pattern with

20–25 Å periodicity represents a stacked skin lipid monolayer with splayed ceramides and chain interdigitation (Figure 3c) (Narangifard et al., 2021), that the lamellar pattern with 55–60 Å periodicity represents a stacked skin lipid bilayer with splayed ceramides and chain interdigitation (Figure 3d) (Narangifard et al., 2021), and that the lamellar pattern with 110–120 Å periodicity represents a stacked skin lipid bilayer with splayed ceramides without chain interdigitation (Figure 3e) (Iwai et al., 2012; Lundborg et al., 2018a).

Reorganization steps of the barrier formation process (Figure 4). Cryo-EM analysis of the skin's barrier formation process suggests that the formation of the skin's barrier structure starts with the secretion of a highly folded and highly hydrated lipid bilayer into the stratum corneum

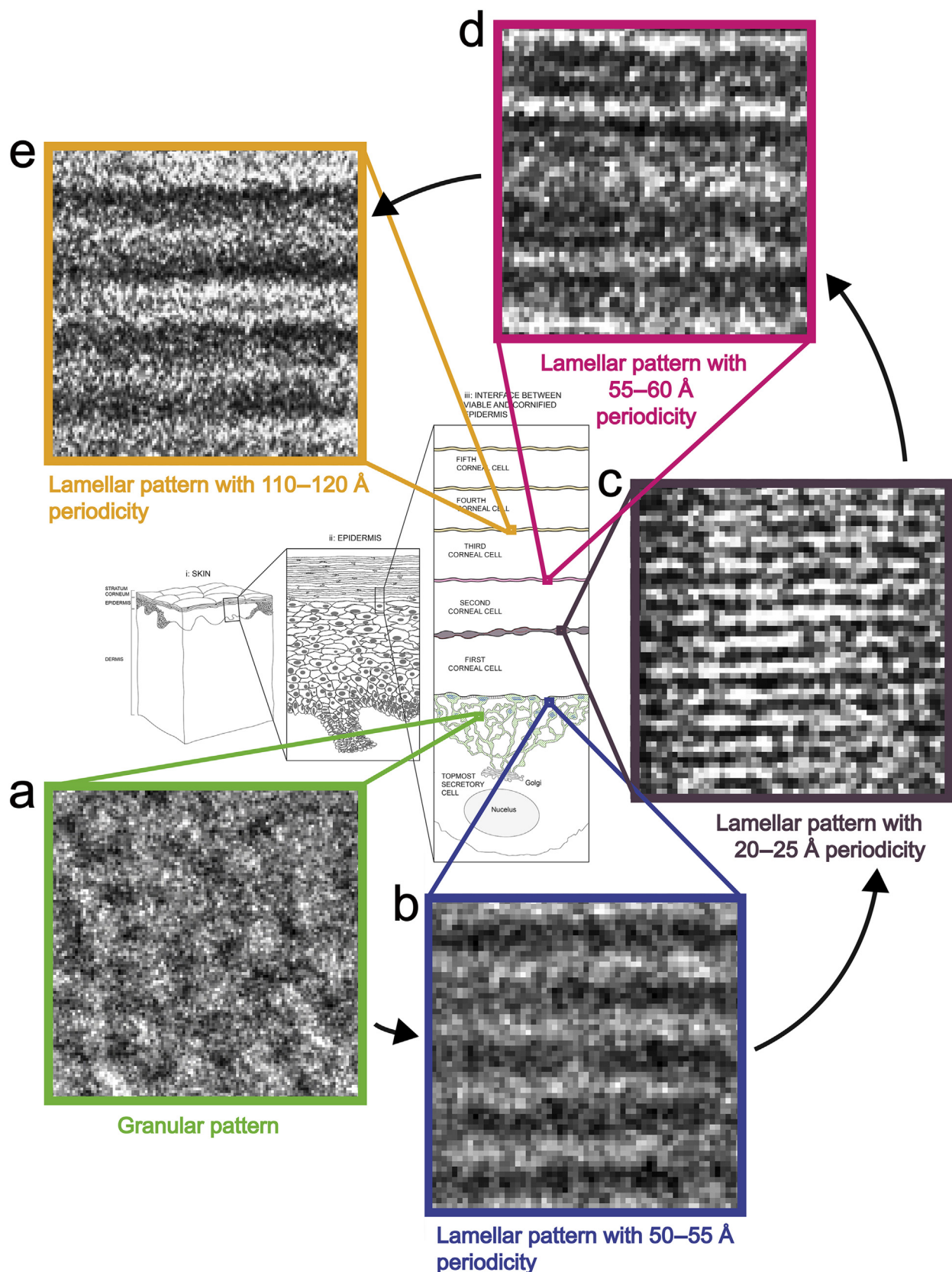


Figure 2. Cryo-EM patterns of the barrier formation process. (a) Granular cryo-EM pattern of the tuboluretticular (lamellar body) network of secretory (SG) cell (green); (b) lamellar cryo-EM pattern with 50–55 Å periodicity of the tuboluretticular network of secretory cell (blue); (c) lamellar cryo-EM pattern with 20–25 Å periodicity of the intercellular space between the first and second corneal (stratum corneum) cells (dark brown); (d) lamellar cryo-EM pattern with 55–60 Å periodicity of the intercellular space between the second and third corneal cells (pink); and (e) lamellar cryo-EM pattern with 110–120 Å periodicity of the intercellular spaces above the third corneal cell (yellow). cryo-EM, cryo-electron microscopy; SG, stratum granulosum.

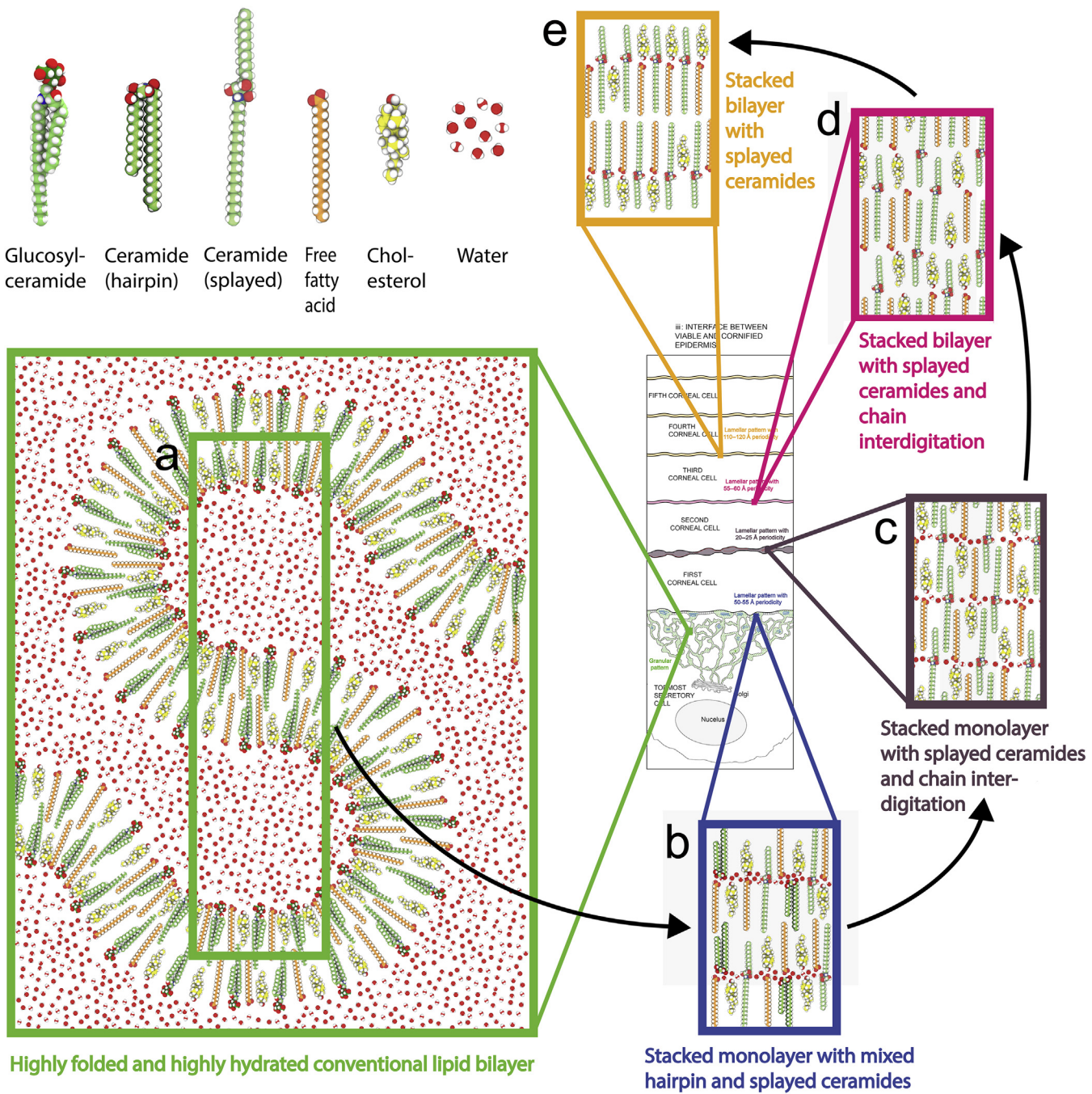


Figure 3. The five stages identified in the barrier formation process. (a) Highly folded and highly hydrated glucosyl-ceramide-based conventional lipid bilayer (green rectangle). (b) Stacked monolayer with mixed hairpin and splayed ceramides (blue rectangle). (c) Stacked monolayer with splayed ceramides and chain interdigitation (dark brown rectangle). (d) Stacked bilayer with splayed ceramides and chain interdigitation (pink rectangle). (e) Stacked bilayer with splayed ceramides without chain interdigitation (yellow rectangle). Molecular color codes: green carbon atoms for glucosyl-ceramide and ceramide molecules, yellow carbon atoms for cholesterol molecules, and orange carbon atoms for free fatty acid molecules. Oxygen (red atoms), hydrogen (white atoms), and nitrogen (dark blue atoms) are colored the same in all lipid molecules and water.

intercellular space (Figure 4a). Cleavage of the sugar groups of glucosyl-ceramides of the lipid bilayer (Figure 4a and b) followed by dehydration (Figure 4b and c) provokes an unfolding or flattening of the folded lipid bilayer, making it collapse into stacks of tightly packed flat lipid bilayers (Figure 4c) (Wennberg et al., 2018).

Once shielded from water, the lipid bilayers' ceramide molecules can now start to stretch out into their preferred

splayed conformation with their two hydrocarbon tails pointing in opposite directions (Figure 4d). When all ceramides have become stretched out (Figure 4e), the system can further relax itself and become more tightly packed by letting the ceramide molecules' short and long hydrocarbon tails as well as the cholesterol and free fatty acid molecules separate into different bands within the layered structure. This internal molecular rearrangement is

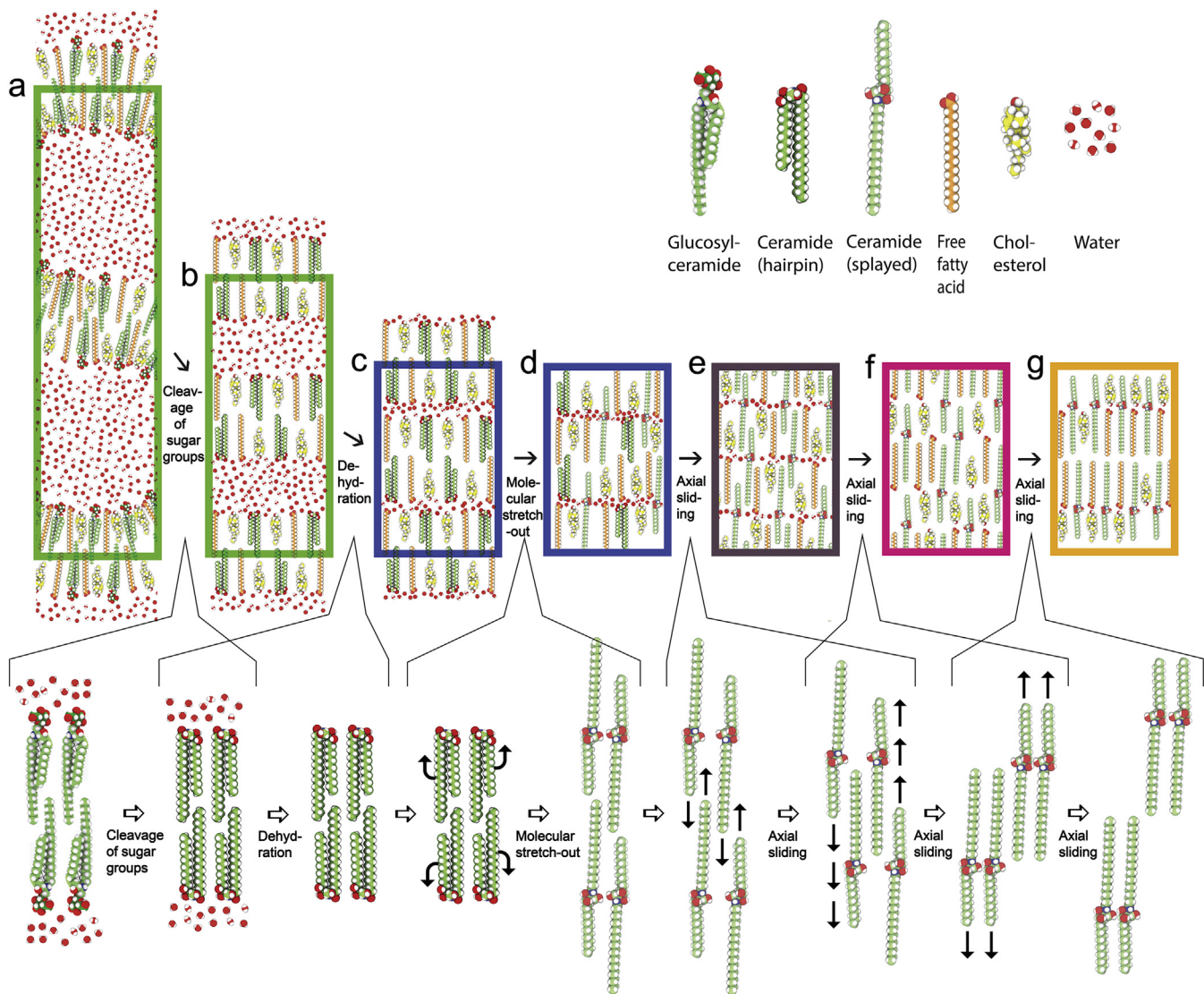


Figure 4. Reorganization steps of the barrier formation process. The lower row indicates (a→b) the cleavage of the sugar groups of glucosyl-ceramides followed by (b→c) dehydration, resulting in a collapse into stacks of tightly packed flat lipid bilayers. (c→d) Ceramide chain flipping resulting in a reorganization of the ceramides from a hairpin (folded) into a splayed (extended) conformation. Sliding along the molecular length axes resulting in (d→e) interdigitation of the lipid chains followed by (e→f) separation of the ceramides' fatty acid and sphingoid chains as well as of the cholesterol and the free fatty acids into different bands of the lamellar structure, and finally, (f→g) uninterdigitation of the lipid chains, yielding (g) the mature skin barrier lipid structure. (a) Highly folded and highly hydrated glucosyl-ceramide-based conventional lipid bilayer (left green rectangle); (b) flattened and highly hydrated stacked ceramide-based conventional lipid bilayer (right green rectangle); (c) stacked lowly hydrated bilayer with hairpin ceramides (left blue rectangle); (d) stacked monolayer with mixed hairpin and splayed ceramides (right blue rectangle); (e) stacked monolayer with splayed ceramides and chain interdigitation (dark brown rectangle); (f) stacked bilayer with splayed ceramides and chain interdigitation (pink rectangle); and (g) stacked bilayer with splayed ceramides without chain interdigitation (yellow rectangle). Molecular color codes: green carbon atoms for glucosyl-ceramide and ceramide molecules, yellow carbon atoms for cholesterol molecules, and orange carbon atoms for free fatty acid molecules. Oxygen (red atoms), hydrogen (white atoms), and nitrogen (dark blue atoms) are colored the same in all lipid molecules and water.

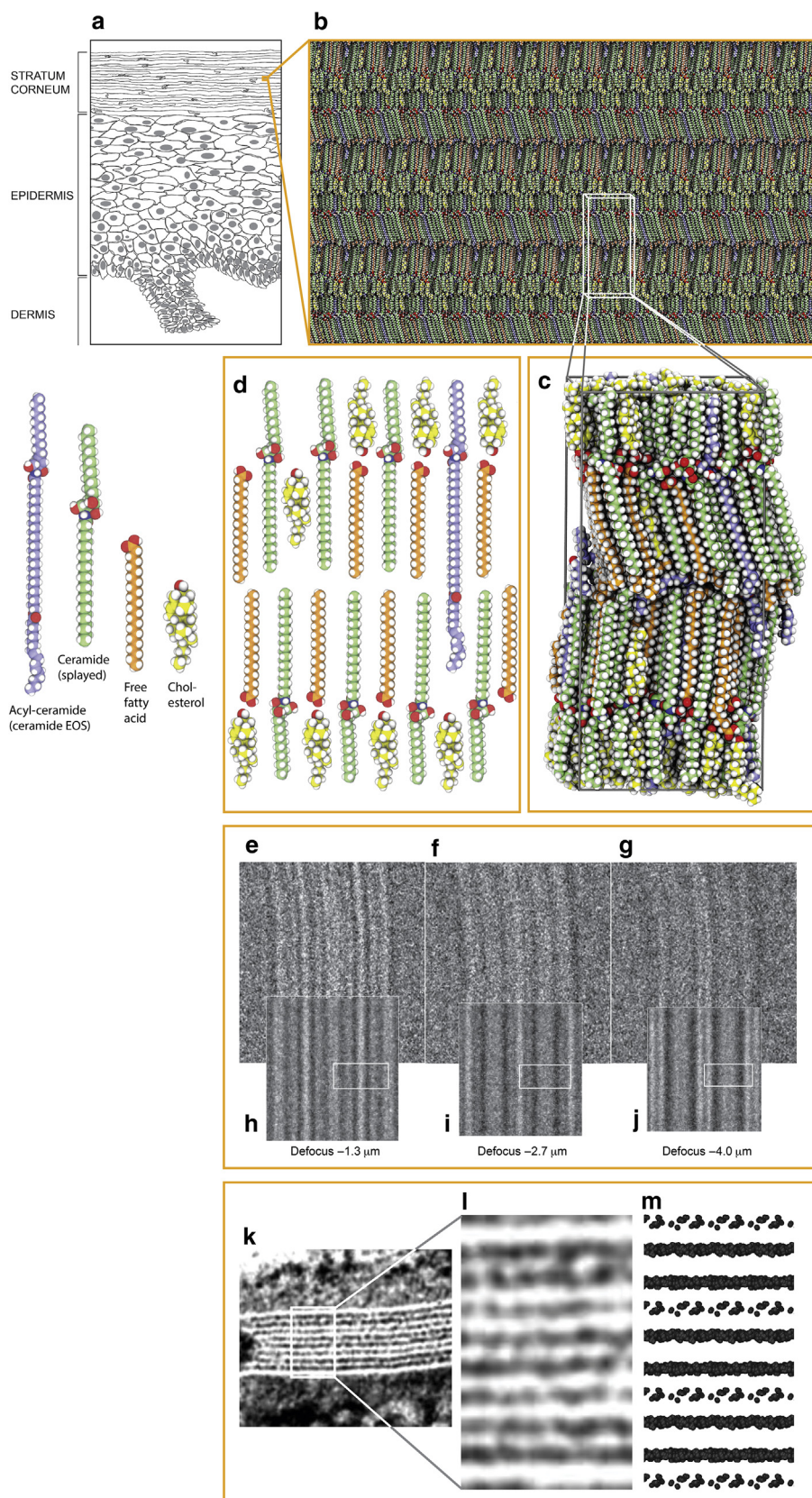
proposed to take place by axial sliding of the ceramide molecules together with associated cholesterol and free fatty acid molecules. The axial sliding process causes initially a lipid chain interdigitation (Figure 4e). Continued axial sliding results in the separation of the ceramides' short and long hydrocarbon tails as well as of the cholesterol and free fatty acid molecules into different bands within the layered structure (Figure 4f). The axial sliding process ends with an uninterdigitation of the lipid chains (Figure 4g), yielding the mature skin barrier structure (Figure 5).

Barrier architecture (Figure 5)

Cryo-EM analysis of the skin's mature barrier structure suggests that it is organized as stacked lipid bilayers of fully stretched (splayed) ceramides with cholesterol largely associated with the ceramides' shorter sphingoid tail and with free fatty acids associated with the ceramides' longer fatty acid tail (Figure 5c and d). Acyl-ceramides (ceramide EOS) (light blue) protrude their ester-bound lignoceric acid ends into the interface between opposing free fatty acid and ceramide fatty acid tail ends. The lignoceric acid ends are mobile and can extend into the opposing layer or fold back into the interface

Figure 5. Architecture of the mature barrier structure. (a) Drawing of epidermis. (b) Atomistic MD model of the mature skin barrier structure. (c) MD simulation box of the model in b. (d) Schematic drawing of the basic molecular arrangement in c: a lipid bilayer of fully stretched (splayed) ceramides with cholesterol (yellow molecules) largely associated with the ceramides' shorter sphingoid side and with free fatty acids (orange molecules) associated with the ceramides' longer fatty acid side. Acyl-ceramides (ceramide EOS) (light blue molecules) protrude their ester-bound lignoceric acid ends into the interface between opposing ceramide fatty acid tail ends. (e–g) Cryo-EM defocus series of the skin's barrier structure. (h–j) Simulated EM defocus series of the model system in b (defocus $-1.3 \mu\text{m}$ for e and h, $-2.7 \mu\text{m}$ for f and i, and $-4.0 \mu\text{m}$ for g and j). The white boxes in h–j represent the position of the simulation box visualized in c. (k) Electron density pattern of the stratum corneum intercellular space in plastic embedded skin stained with RuO₄, graciously obtained from Dr Philip Wertz and adapted from Madison et al. (1987). (l) Enlarged view of the area marked by a white box in k. (m) Van der Waals representation of oxygens and nitrogens (the most electronegative atoms in the system) of the model system in b. (m) is a rough estimate of what the electron density pattern of the model system in b would look like after RuO₄ staining. (e–m) Figures are adapted from Lundborg et al. (2018a). Molecular color codes: green carbon atoms for ceramide molecules, light-blue carbon atoms for acyl-ceramide molecules, yellow carbon atoms for cholesterol molecules, and orange carbon atoms for free fatty acid molecules. Oxygen (red atoms), hydrogen (white atoms), and nitrogen (dark blue atoms) are colored the same in all lipid molecules and water.

cryo-EM, cryo-electron microscopy; MD, molecular dynamics; RuO₄, ruthenium tetroxide.



between the layers. Another feature is that the acyl-ceramides' ester groups make the interface between the ceramides' fatty acid tail ends more polar than the interface between the ceramides' sphingoid tail ends (Figure 5c and d). This arrangement offers a tight and robust barrier structure and is compatible both with cryo-EM (Figure 5e–j) and with the broad-narrow-broad electron-lucent RuO₄ staining band pattern observed using conventional EM (Hou et al., 1991; Madison et al., 1987) (Figure 5k–m).

Future perspective

Having access to a near-native reference from healthy skin, it may now be possible to investigate the deviations in lipid structure that could underlie barrier dysfunction in skin diseases such as atopic dermatitis, psoriasis, and the ichthyoses.

The knowledge on the structure of the skin's permeability barrier may facilitate physics-based skin permeability calculations using MD simulation (Lundborg et al., 2018b). This may aid in predicting the properties of drugs interacting with the skin and optimizing them for topical and percutaneous drug delivery. In addition, it may be used for skin toxicity assessment.

The experimental approach exemplified in this paper, consisting in obtaining *in situ* a near-native structural reference of a biomolecular complex using cryo-EM (CEMOVIS) combined with MD modeling and EM simulation, may be followed by more detailed analysis *ex situ* and *in silico* using, for example, X-ray crystallography, single-particle cryo-EM, nuclear magnetic resonance spectroscopy, or MD simulation. It may thus be useful for examining the molecular-level structure/function relationships of biostructures inside any cell or tissue within the constraints of a near-native reference.

ORCIDs

Lars Norlén: <http://orcid.org/0000-0002-8049-2556>
 Magnus Lundborg: <http://orcid.org/0000-0002-0873-7854>
 Christian Wennberg: <http://orcid.org/0000-0003-4012-1678>
 Ali Narangifard: <http://orcid.org/0000-0003-3044-0827>
 Bertil Daneholt: <http://orcid.org/0000-0001-8589-5373>

CONFLICT OF INTEREST

The authors state no conflict of interest.

ACKNOWLEDGMENTS

This work was made possible by the generous support from the Swedish Medical Society, Oriflame, Shiseido Japan, LEO Pharma, Wenner-Gren Foundation, the Swedish eScience Research Center, the Welander foundation, and ERCO Pharma. The service of the Core Facility for Electron Tomography at Karolinska Institutet as well as the resources provided by the Swedish National Infrastructure for Computing at PDC Centre for High-Performance Computing are acknowledged.

AUTHOR CONTRIBUTIONS

Conceptualization: LN; Writing: LN, ML, CW, AN, BD

REFERENCES

- Al-Amoudi A, Chang JJ, Leforestier A, McDowell A, Salamin LM, Norlén LP, et al. Cryo-electron microscopy of vitreous sections. *EMBO J* 2004;23: 3583–8.
- Berenson GS, Burch GE. Studies of diffusion of water through dead human skin; the effect of different environmental states and of chemical alterations of the epidermis. *Am J Trop Med Hyg* 1951;31:842–53.
- Blank IH. Factors which influence the water content of the stratum corneum. *J Invest Dermatol* 1952;18:433–40.
- Bouwstra JA, Gooris GS, Dubbelaar FE, Weerheim AM, Ijzerman AP, Ponec M. Role of ceramide 1 in the molecular organization of the stratum corneum lipids. *J Lipid Res* 1998;39:186–96.
- Bouwstra JA, Gooris GS, van der Spek JA, Bras W. Structural investigations of human stratum corneum by small-angle X-ray scattering. *J Invest Dermatol* 1991;97:1005–12.
- Breathnach AS, Goodman T, Stolinski C, Gross M. Freeze-fracture replication of cells of stratum corneum of human epidermis. *J Anat* 1973;114:65–81.
- Brody I. Intercellular space in normal human stratum corneum. *Nature* 1966;209:472–6.
- Brody I. A light and electron microscopy study of normal human stratum corneum with particular reference to the intercellular space. *Ups J Med Sci* 1989;94:29–45.
- den Hollander L, Han H, Winter M, Svensson L, Masich S, Daneholt B, et al. Skin lamellar bodies are not discrete vesicles but part of a tubuloreticular network. *Acta Derm Venereol* 2016;96:303–8.
- Dubochet J, Adrian M, Chang JJ, Homo JC, Lepault J, McDowell AW, et al. Cryo-electron microscopy of vitrified specimens. *Q Rev Biophys* 1988;21: 129–228.
- Durieu F. Recherches expérimentales sur l'absorption et l'exhalation par le tégument externe. *Arch Gen Med T* 1856;7:161–73.
- Elias PM. Epidermal lipids, barrier function, and desquamation. *J Invest Dermatol* 1983;80(Suppl. 1):S44–9.
- Elias PM, Cullander C, Mauro T, Rassner U, Kömuves L, Brown BE, et al. The secretory granular cell: the outermost granular cell as a specialized secretory cell. *J Investig Dermatol Symp Proc* 1998;3:87–100.
- Elias PM, Friend DS. The permeability barrier in mammalian epidermis. *J Cell Biol* 1975;65:180–91.
- Fartasch M. Epidermal barrier in disorders of the skin. *Microsc Res Tech* 1997;38:361–72.
- Feingold KR, Elias PM. Role of lipids in the formation and maintenance of the cutaneous permeability barrier. *Biochim Biophys Acta* 2014;1841:280–94.
- Forslind B. A domain mosaic model of the skin barrier. *Acta Derm Venereol* 1994;74:1–6.
- Homolle A. Expériences physiologiques sur l'absorption par la tégument externe chez l'homme dans le bain. *Union Med* 1853;7:462.
- Hou SY, Mitra AK, White SH, Menon GK, Ghadially R, Elias PM. Membrane structures in normal and essential fatty acid-deficient stratum corneum: characterization by ruthenium tetroxide staining and X-ray diffraction. *J Invest Dermatol* 1991;96:215–23.
- Iwai I, Han H, den Hollander L, Svensson S, Ofverstedt LG, Anwar J, et al. The human skin barrier is organized as stacked bilayers of fully extended ceramides with cholesterol molecules associated with the ceramide sphingoid moiety. *J Invest Dermatol* 2012;132:2215–25.
- Landmann L. Epidermal permeability barrier: transformation of lamellar granule-disks into intercellular sheets by a membrane-fusion process, a freeze-fracture study. *J Invest Dermatol* 1986;87:202–9.
- Lavker RM. Membrane coating granules: the fate of the discharged lamellae. *J Ultrastruct Res* 1976;55:79–86.
- Lundborg M, Narangifard A, Wennberg CL, Lindahl E, Daneholt B, Norlén L. Human skin barrier structure and function analyzed by cryo-EM and molecular dynamics simulation. *J Struct Biol* 2018a;203:149–61.
- Lundborg M, Wennberg CL, Narangifard A, Lindahl E, Norlén L. Predicting drug permeability through skin using molecular dynamics simulation. *J Control Release* 2018b;283:269–79.
- Madison KC, Sando GN, Howard EJ, True CA, Gilbert D, Swartzendruber DC, et al. Lamellar granule biogenesis: a role for ceramide glucosyltransferase, lysosomal enzyme transport, and the Golgi. *J Investig Dermatol Symp Proc* 1998;3:80–6.
- Madison KC, Swartzendruber DC, Wertz PW, Downing DT. Presence of intact intercellular lipid lamellae in the upper layers of the stratum corneum. *J Invest Dermatol* 1987;88:714–8.
- Matoltsy AG. Membrane-coating granules of the epidermis. *J Ultrastruct Res* 1966;15:510–5.
- Narangifard A, Wennberg CL, den Hollander L, Iwai I, Han H, Lundborg M, et al. Molecular reorganization during the formation of the human skin barrier studied *in situ*. *J Invest Dermatol* 2021;141:1243–53.e6.
- Narangifard A, den Hollander L, Wennberg CL, Lundborg M, Lindahl E, Iwai I, et al. Human skin barrier formation takes place via a cubic to lamellar lipid phase transition as analyzed by cryo-electron microscopy and EM-simulation. *Exp Cell Res* 2018;366:139–51.

- Odlund GF, Holbrook K. The lamellar granules of epidermis. *Curr Probl Dermatol* 1981;9:29–49.
- Onken HD, Moyer CA. The water barrier in human epidermis. Physical and chemical nature. *Arch Dermatol* 1963;87:584–90.
- Potts RO, Guy RH. Predicting skin permeability. *Pharm Res* 1992;9:663–9.
- Rabionet M, Gorgas K, Sandhoff R. Ceramide synthesis in the epidermis. *Biochim Biophys Acta* 2014;1841:422–34.
- Schaefer H, Redelmeier TE. Skin barrier: principles of percutaneous absorption. Basel, Switzerland: Karger Publishers; 1996.
- Scheuplein RJ, Blank IH. Permeability of the skin. *Physiol Rev* 1971;51:702–47.
- Schmitt T, Neubert RHH. State of the art in stratum corneum research: the biophysical properties of ceramides. *Chem Phys Lipids* 2018;216:91–103.
- van Smeden J, Janssens M, Gooris GS, Bouwstra JA. The important role of stratum corneum lipids for the cutaneous barrier function. *Biochim Biophys Acta* 2014;1841:295–313.
- Wennberg CL, Narangifard A, Lundborg M, Norlén L, Lindahl E. Structural transitions in ceramide cubic phases during formation of the human skin barrier. *Biophys J* 2018;114:1116–27.
- Wertz P. Epidermal lamellar granules. *Skin Pharmacol Physiol* 2018;31:262–8.
- Wertz PW, Downing DT. Ceramides of pig epidermis: structure determination. *J Lipid Res* 1983;24:759–65.
- Winsor TB, Burch GE. Differential roles of layers of human epigastric skin on diffusion rate of water. *Arch Intern Med* 1944;74:428–36.
- Yamanishi H, Soma T, Kishimoto J, Hibino T, Ishida-Yamamoto A. Marked changes in lamellar granule and trans-Golgi network structure occur during epidermal keratinocyte differentiation. *J Invest Dermatol* 2019;139:352–9.
- Yokouchi M, Atsugi T, van Logtestijn M, Tanaka RJ, Kajimura M, Suematsu M, et al. Epidermal cell turnover across tight junctions based on Kelvin's tetrakaidecahedron cell shape. *Elife* 2016;5:e19593.



This work is licensed under a Creative Commons Attribution 4.0 International License. To view a copy of this license, visit <http://creativecommons.org/licenses/by/4.0/>